Communications to the Editor

Influence of Shear on the Hexagonal-to-Disorder Transition in a Diblock Copolymer Melt

Frank S. Bates,* Kurt A. Koppi, and Matthew Tirrell

Department of Chemical Engineering and Materials Science, University of Minnesota, Minneapolis, Minnesota 55455

Kristoffer Almdal and Kell Mortensen

Risø National Laboratory, DK-4000 Roskilde, Denmark

Received March 28, 1994
Revised Manuscript Received July 5, 1994

The qualitative effects of deformation and flow on well-ordered block copolymers have been recognized for at least two decades.[1,2] Yet only recently have hydrodynamic fields (primarily shearing deformations) been exploited in studying the fundamental nature of block copolymer phase behavior.[3-11] Similar advances have occurred in several related areas including liquid crystals,[12] surfactants,[13] colloidal suspensions,[14] and polymer solutions and blends,[15] all of which exhibit a strong coupling between large strain deformation and local microstructure. These developments in the emerging field of "soft materials" mimic the early stages of research with solid-state compounds, where magnetic and electrical fields were applied to the investigation of various phase behaviors such as superconductivity and magnetism. As with the classical solid-state techniques, the application of a flow field to soft matter is particularly effective when combined with a structural probe such as X-ray or neutron scattering.

Mindful of the opportunities that would be created by combining shear deformation with small-angle neutron scattering (SANS), we recently developed a dynamic shearing device that could be operated *in situ* while SANS measurements were conducted on block copolymer melts. We opted for a simple reciprocating shearing mode, rather than the couette geometry,[12-15] where the neutron beam is directed normal to the plane of shear. This design greatly simplifies sample loading while affording a wide range of strain amplitudes (typically from 1 to 1000%) and shear rates. The polymer is held between aluminum plates that are mounted onto thermostated (±1 °C) brass blocks, one of which is held fixed while the other translates at a steady speed. Adjustable reversing switches set the travel distance (i.e., strain amplitude). A detailed description of this instrument is provided elsewhere.[16]

We have been conducting a systematic investigation of diblock copolymer melts as a function of shear rate, ($|\dot{\gamma}| = \partial\gamma/\partial t$), strain amplitude ($|\gamma|$), temperature, and composition (f) in the vicinity of order–disorder and order–order phase transitions. Previous publications have dealt with the lamellar-to-disorder,[6,7] cylinders (hexagonal)-to-spheres (bcc),[17] and intermediate hexagonal phases between lamellae and cylinders.[8] In this article we report our initial findings for a poly(ethylene-propylene)–poly(ethylethylene) (PEP–PEE) specimen that undergoes a hexagonal-to-disorder transition in the absence of shear (i.e., $|\dot{\gamma}| = 0$). The synthesis, molecular characterization, and rheological and structural features of this material have been reported earlier.[11] This deuterium-labeled polymer, referred to as PEP–PEE-7, contains 77% by volume PEP, an overall molecular weight of $\bar{M}_n = 1.0 \times 10^5$ (on a hydrogeneous equivalent basis), and $\bar{M}_w/\bar{M}_n = 1.07$. Neutron contrast is provided by a 75% deuterium-labeled PEE block. The order–disorder transition (ODT) occurs at 155 ± 1 °C under field free ($|\dot{\gamma}| = 0$) conditions.

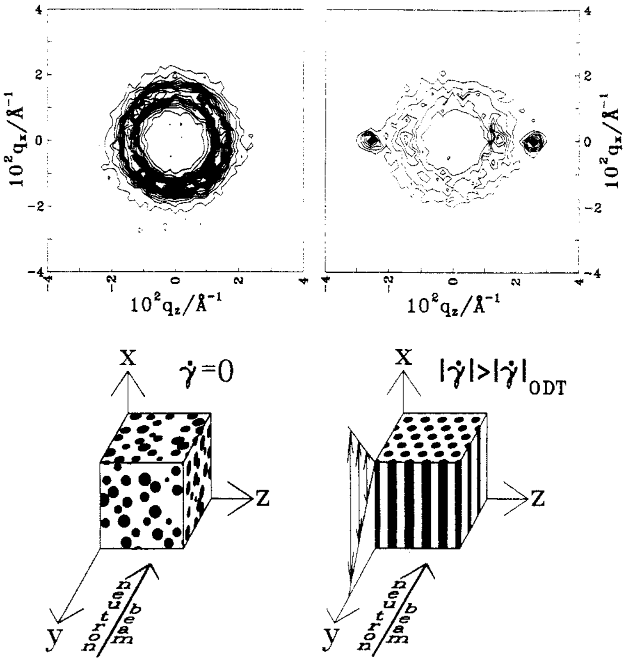

Figure 1. Contour plots of SANS data obtained from sample PEP–PEE-7 at 157 °C. The contour lines indicate constant linear increments of intensity. The azimuthally symmetric scattering ring obtained without shear ($\dot{\gamma} = 0$) is associated with the fluctuating disordered morphology depicted on the lower left. Application of a reciprocating shearing field ($|\dot{\gamma}| = 6\ \text{s}^{-1}$ with shear direction and gradient along x and y, respectively) produced the strong reflections seen in the other contour plot, which derives from oriented hexagonally packed cylinders, as illustrated on the lower right.

SANS experiments were conducted at the Risø National Laboratory in Denmark using $\lambda = 6.1$ Å wavelength neutrons ($\Delta\lambda/\lambda = 0.09$) and a 6 m sample-to-detector distance. Scattered neutrons were recorded with an area detector and are reported in arbitrary units of intensity. Experiments reported here were performed with a 0.3 mm gap, $|\gamma| \cong 300\%$, and a shear rate of 6 s^{-1}. In order to guard against sample degradation the shearing device was operated within a helium-filled environmental chamber. An illustration identifying the deformation and neutron beam orientations is given in Figure 1. This schematic also depicts the two steady-state microstructures that will be dealt with in this article.

Two temperatures, T = 157 and 162 °C, have been selected to demonstrate the effects of shear on PEP–PEE-7 above T_{ODT} ($\dot{\gamma} = 0$); a full report containing data obtained at numerous temperatures and shear rates, and with heating and cooling of the specimen, will be presented in a future publication. In the absence of shear the material exists in a fluctuating disordered state. This is evidenced by an azimuthally symmetric scattering pattern that contains a well-defined ring of intensity at $|\mathbf{q}| = q^*$ (where

0024-9297/94/2227-5934$04.50/0

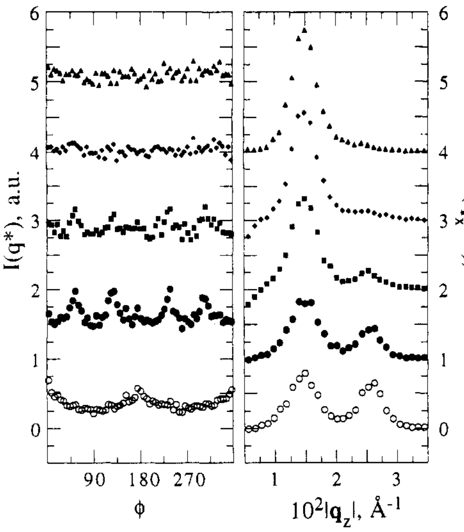

Figure 2. Time evolution of SANS patterns upon cessation of shearing ($|\dot{\gamma}| = 6$ s^{-1}) at 157 °C: (a, left) azimuthal dependence of the intensity contained within the anulus centered on q^*; (b, right) angular dependence of the intensity defined by the rectangular band $|q_x| \leq 0.004$ Å^{-1}. The first set of data (○) was obtained during 30 s of counting, while shearing, and corresponds to the contour plot to the right in Figure 1. After shearing was stopped, successive data sets were obtained in 50 s intervals (30 s counting and 20 s data transfer). These are progressively shifted vertically by 1 intensity unit. Appearance of the four-peak structure in $I(q^*, \phi)$ along with the reflection at $|\mathbf{q}_z| = \sqrt{3}q^*$ is indicative of an undulating cylinder morphology.

$|\mathbf{q}| = 4\pi\lambda^{-1} \sin(\theta/2)$), as shown for $T = 157$ °C in Figure 1 (top left). Upon turning on the $|\dot{\gamma}| = 6$ s^{-1} field, the material rapidly transforms into an oriented hexagonal cylinder phase, which is evidenced by the development of well-defined Bragg reflections, as seen in the contour plot of Figure 1 (top right). This process is completely reversible and the isotropic pattern is fully recovered soon after the shear field is switched off (see below). In our earlier work with PEP–PEE-7[11] we established that the (10) plane of the hexagonal crystal structure aligns parallel to the plane of shear with the cylinder axis coincident with the shear direction, as sketched in Figure 1. The (11) reflections at $|\mathbf{q}| = \sqrt{3}q^*$ confirm this orientation in the present case.

Our 2-dimensional scattering patterns can be characterized using two data reduction schemes. In the first, the azimuthal dependence $I(q^*, \phi)$ is obtained by averaging the intensities over a narrow band of scattering wavevectors centered on q^*, 0.011 Å^{-1} < $|\mathbf{q}|$ < 0.019 Å^{-1}. A rectangular band defined by $|\mathbf{q}_x| \leq 0.004$ Å^{-1} is used to produce plots of $I(|\mathbf{q}_z|)$ in the second method. The results of these averaging procedures for the two contour plots found in Figure 1 are included in Figure 2a,b respectively. In the absence of shear at 157 °C (upper data sets) $I(q^*, \phi)$ is featureless and $I(|\mathbf{q}_z|)$ contains a single broad peak at q^*. Under shear (lower data sets), the former is ϕ dependent, and a prominent $\sqrt{3}q^*$ reflection appears in $I(|\mathbf{q}_z|)$. Similar results are obtained at $T = 162$ °C, as shown by the upper and lower data sets of Figure 3. At both temperatures the overall intensity at q^* increases when the material disorders. Clearly, dynamic shear *increases* the hexagonal-to-disorder transition temperature in this diblock copolymer melt.

Along with these equilibrium (or steady-state) results, we have discovered an interesting transient response when the shear field is abruptly switched off. The limiting factors in characterizing the isothermal transition from the shear-induced ordered state to the field-free disordered state are the times required to (i) require acceptable statistics and (ii) transfer the information from the detector to permanent storage. Owing to the excellent contrast in PEP–PEE-7, we were able to perform relatively fast experiments: 30 s data acquisition and 20 s data transfer times, for a total cycle time of 50 s.

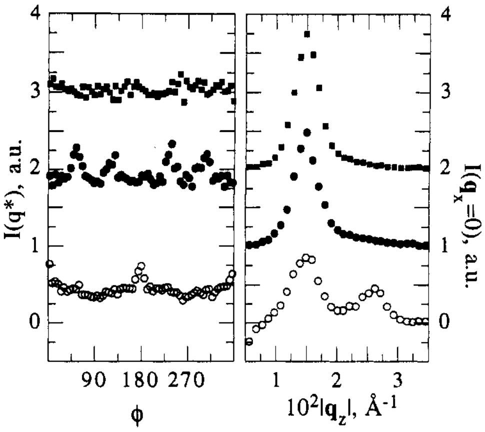

Figure 3. SANS data for time evolution experiments conducted at 162 °C. The data were obtained and treated in the same manner described in Figure 2. Here the four-peak pattern in $I(q^*, \phi)$ is not accompanied by a reflection at $|\mathbf{q}_z| = \sqrt{3}q^*$, which is evidence for a bcc-ordered spherical phase. The ϕ dependence of the four (110) peaks is consistent with epitaxial growth of the cubic phase from oriented hexagonally packed cylinders.

A representative set of results, obtained during a 200 s period following cessation of shearing at 157 °C is presented in Figure 2. In the first 30 s data acquisition period a distinct four-peak structure develops in $I(q^*, \phi)$ with a corresponding increase and decrease in $I(|\mathbf{q}_z| = q^*)$ and $I(|\mathbf{q}_z| = \sqrt{3}q^*)$, respectively. Within approximately four cycles (200 s) these features disappear, leaving the equilibrium fluctuating state. The transient response at 162 °C (Figure 3) is noticeably different. In the first 30 s data acquisition period a similar four-peak pattern appears in $I(q^*, \phi)$, but the $I(|\mathbf{q}_z| = \sqrt{3}q^*)$ reflection has disappeared entirely. After just two cycles (100 s) the sample has reached the disordered isotropic state. At 164 °C the transient structure decayed faster than could be recorded within the experimental time constraints, while at 156 °C (T_{ODT} + 1 °C) evidence of the four-peak pattern and $\sqrt{3}q^*$ reflection persisted for roughly 8 or 9 cycles (≈400 s). A comprehensive treatment of these results will be provided in a future publication.

On the basis of our recent work with $f = 0.25$ and 0.83 PEP–PEE diblock copolymers, which exhibit static ($|\dot{\gamma}| = 0$) thermally induced hexagonal-to-bcc order–order transitions,[17] we can deduce a simple, and rather compelling, interpretation of the SANS patterns associated with the disordering of shear-aligned cylinders. In separate reports[10,17] we have shown that the bcc spherical microstructure grows expitaxially from the hexagonal cylinder phase, with the [$\bar{1}$11] direction parallel to the cylinder axis (i.e., the 6-fold hexagonal axis transforms into a 3-fold cubic axis).[17] If the cylindrical phase is aligned, then this epitaxy places the [110] direction along the original shear gradient, coincident with the neutron beam direction in the dynamic SANS experiment (see Figure 1). Since there are two degenerate epitaxial orientations, two equivalent structures evolve, leading to four {110} reflections located at $\phi = \pm 35.3°$ relative to the shear direction.[10] This is precisely what is found in Figures 2 and 3.

Such a pattern establishes a symmetry, but not a microstructure. Two microstructures, depicted in Figure 4, seem most plausible: an undulating cylinder state or spheres. In fact we believe that both structures occur,

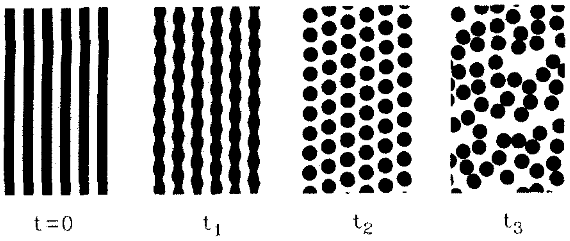

Figure 4. Schematic representation of the transition from hexagonally ordered cylinders to disorder following cessation of shearing. At 157 °C the sequence $\tau_1 \rightarrow \tau_3$ is postulated while at 162 °C $(\tau_1) \rightarrow \tau_2 \rightarrow \tau_3$ is indicated.

where the discriminating feature is the $|\mathbf{q}_z|$ reflection at $\sqrt{3}q^*$ (Figures 2b and 3b). For the bcc phase $\sqrt{3}q^*$ reflections derive from the family of $[11\bar{2}]$ planes, which are not orthogonal to [110], i.e., the shear (or x–z) plane in Figure 1. Hence, when fully transformed to the epitaxial bcc spherical morphology, the $|\mathbf{q}_z| = \sqrt{3}q^*$ reflection disappears,[10,17] as is found at 162 °C (Figure 3). Conversely, in an undulating (hexagonal) cylinder state the $\sqrt{3}q^*$ reflections would persist. At 157 °C loss of the four azimuthal reflections at q^* coincides with the disappearance of the $\sqrt{3}q^*$ peak, and we associate this transient state with the ordered undulations depicted in Figure 4.

These results make contact with a number of theoretical and experimental studies involving soft materials. We have established that shear *increases* the hexagonal-to-disorder transition temperature in diblock copolymer melts, analagous to what occurs in the lamelar (i.e., symmetric) case. This result is anticipated by the theoretical work of Marques and Cates.[18] However, Winter et al.[5] report a *suppression* of T_{ODT} when a triblock copolymer melt is sheared, raising the intriguing possibility of a molecular architecture dependence to the field susceptibility.

Perhaps the most provocative conclusions of this work involve the nature of fluctuations near the ODT for asymmetric block copolymer melts. A shear field destroys fluctuations (anisotropically), thereby making the system more mean-field-like, which is why T_{ODT} increases.[18] The transient states accessed during the shear-quench experiments provide a unique glimpse at the fluctuation symmetry, as well as the underlying mean-field structure, in both the ordered and disordered states. When the field is quenched at 157 °C, fluctuations develops in the form of undulations (with bcc symmetry) on the hexagonal lattice. [In a forthcoming publication we will show that these fluctuations are also present at equilibrium as $T \rightarrow T_{\mathrm{ODT}}$ when $|\dot{\gamma}| = 0$]. We believe such anisotropic fluctuations play a key role in creating complex ordered phases near the hexagonal–lamellar transitions[8] and may represent a soft-material analogue of the soft modes found in solid-state compounds.[19] Here the reader is referred to the seminal theoretical work of Brazovskii et al.[20] At 162 °C we find that the transition from the mean-field-like (i.e., sheared) hexagonal phase to disorder occurs via a bcc sphere state. This is precisely what Leibler[21] anticipated in his original mean-field treatment of block copolymers near the ODT. Naturally, the bcc phase will not be stable under large amplitude shearing, even in the mean-field limit. Thus, our results provide strong support for both the mean-field concept[22] and the Brazovskii[22] fluctuation corrections introduced by Fredrickson and Helfand.[23]

Moreover, these transient structures point to a field-free ($|\dot{\gamma}| = 0$) fluctuating state that resembles a disordered (i.e., melted) spherical phase, as depicted in Figure 1, rather than the wormlike morphology that is encountered in some surfactant systems.[24] Consistent with this reasoning, a nematic cylinder phase has not been predicted, nor found experimentally, in block copolymer melts, although these results do not preclude such an event. The picture that emerges from this analysis is a disordered state near the ODT that is truly isotropic, for all f. When $f \rightarrow 0$ or 1 the fluctuations near the ODT resemble disordered spheres. In the symmetric limit, $f = {}^1/_2$, a disordered bicontinuous morphology must exist, probably resembling a spinodal structure.[25] A continuous crossover between these limits is indicated by our results and analysis.

In summary, we have shown that dynamic shear increases the hexagonal-to-disorder transition temperature in an asymmetric PEP–PEE diblock copolymer melt. Disordering the shear-induced hexagonal phase, following field quenching, proceeds via a transient undulating cylinder or bcc spherical state. These results support the concept of shear-induced mean-field behavior and point to locally isotropic fluctuations in the disordered state.

Acknowledgment. This research was supported by the Center for Interfacial Engineering (CIE), an NSF sponsored Engineering Research Center at the University of Minnesota, and the Air Force Office of Scientific Research (AF/F 49620-93). F.S.B. and K.A. also benefitted from a NATO Travel Grant.

References and Notes

(1) Keller, A.; Pedemonte, E.; Willmouth, F. M. *Nature* **1970**, *225*, 538.
(2) Hadziioannou, G.; Mathis, A.; Skoulios, A. *Colloid Polym. Sci.* **1979**, *257*, 136.
(3) Hadziioannou, G.; Picot, C.; Skoulios, A.; Ionescu, M.-L.; Mathis, A.; Dupplessix, R.; Gallot, Y.; Lingelser, J.-P. *Macromolecules* **1982**, *15*, 263.
(4) Morrison, F. A.; Mays, J. W.; Muthukumar, M.; Nakatani, A. I.; Han, C. C. *Macromolecules* **1993**, *26*, 5271.
(5) Winter, H. H.; Scott, D. B.; Gronski, W.; Okamoto, S.; Hashimoto, T. *Macromolecules* **1993**, *26*, 7236.
(6) Koppi, K. A.; Tirrell, M.; Bates, F. S. *Phys. Rev. Lett.* **1993**, *70*, 1449.
(7) Koppi, K. A.; Tirrell, M.; Bates, F. S.; Almdal, K. A.; Colby, R. H. *J. Phys. II, Fr.* **1992**, *2*, 1941.
(8) Hamley, I. W.; Koppi, K. A.; Rosedale, J. H.; Bates, F. S.; Almdal, K.; Mortensen, K. *Macromolecules* **1993**, *26*, 5959.
(9) Almdal, K.; Koppi, K. A.; Bates, F. S.; Mortensen, K. *Macromolecules* **1992**, *25*, 1743.
(10) Almdal, K.; Koppi, K. A.; Bates, F. S. *Macromolecules* **1993**, *26*, 4058.
(11) Almdal, K.; Bates, F. S.; Mortensen, K. *J. Chem. Phys.* **1992**, *96*, 9122.
(12) Safinya, C. R.; Sirota, E. B.; Plano, R. J. *Phys. Rev. Lett.* **1991**, *66*, 3004.
(13) Penfold, J.; Staples, E.; Cummins, P. G. *Adv. Colloid Interfacial Sci.* **1991**, *34*, 451.
(14) Chen, L. B.; Zukoski, C. F.; Ackerson, B. J.; Hanley, H. J. M.; Straty, G. C.; Barker, J.; Glinka, C. J. *Phys. Rev. Lett.* **1992**, *69*, 688.
(15) Dixon, P. K.; Pine, D. J.; Wu, X.-L. *Phys. Rev. Lett.* **1992**, *68*, 2239; Hobbie, E. K.; Hair, D. W.; Nakatani, A. I.; Han, C. C. *Phys. Rev. Lett.* **1992**, *69*, 1951.
(16) Koppi, K. A. Ph.D. Thesis, Department of Chemical Engineering and Materials Science, University of Minnesota, 1993.
(17) Koppi, K. A.; Tirrell, M.; Bates, F. S.; Almdal, K.; Mortensen, K. *J. Rheol.* **1994**, *38*, 999.
(18) Marques, C. M.; Cates, M. E. *J. Phys. (Paris)* **1990**, *51*, 1733.
(19) *Topics in Current Physics*; Müller, K. A., Thomas, H., Eds.; Springer: Berlin, Heidelberg, New York, 1991; Vol. 45. *Ibid.*, 1981; Vol. 23.
(20) Brazovskii, S. A.; Dzyaloshinskii; Muratov, A. R. *Zh. Eksp. Teor. Fiz.* **1987**, *93*, 1110; *Sov. Phys. JETP* **1987**, *66*, 625.
(21) Leibler, L. *Macromolecules* **1980**, *13*, 1602.
(22) Brazovskii, S. *Eksp. Teor. Fiz.* **1975**, *68*, 175; *Sov. Phys. JETP* **1975**, *41*, 85.
(23) Fredrickson, G. H.; Helfand, E. *J. Chem. Phys.* **1988**, *89*, 5890.
(24) Lin, Z.; Scriven, L. E.; Davis, H. T. *Langmuir* **1992**, *8*, 2200. Cummins, P. G.; Staples, E.; Hayter, J. B.; Penfold, *J. Chem. Soc., Faraday Trans.* **1987**, *83*, 2773.
(25) Bates, F. S.; Rosedale, J. H.; Fredrickson, G. H. *J. Chem. Phys.* **1990**, *92*, 6255.